United States Department of Agriculture

NRCS

Natural Resources Conservation Service
National Soil Survey Center
Federal Building, Room 152
100 Centennial Mall North
Lincoln, NE 68508-3866

Phone: (402) 437-5499
FAX: (402) 437-5336

SUBJECT: MGT – Geophysical Assistance

June 7, 2013

TO: Michelle Lohstroh
Acting State Conservationist
NRCS, Columbus, Ohio

File Code: 330-20-7

Purpose:
The objective of this study was to evaluate the use of geophysical methods for Ohio soil survey and technical services including the Wetland Reserve Program (eligibility and restoration issues).

Principal Participants:
LaRae Baker, Soil Conservationist, NRCS, Bellefontaine, OH
Steven Baker, State Soil Scientist, NRCS, Columbus, OH
Chris Davis, Soil Scientist, NRCS, Findlay, OH,
Jim Doolittle, Research Soil Scientist, NRCS, NSSC, Newtown Square, PA
Jeff Glanville, Soil Scientist/Soil Database Manager, NRCS, Columbus, OH
Charles Hanner, Soil Scientist, NRCS, Findlay, OH
Melissa Hanner, Soil Scientist, NRCS, Tiffin, OH
Neil Martin, Soil Scientist, NRCS, Findlay, OH,
Donald McClure, Soil Scientist, NRCS, Findlay, OH
Chad Meenach, Civil Engineering Technician, NRCS, Marion, OH

Activities:
All field activities were completed on May 14-16, 2013.

Summary:

1. In Ohio, drainage pipes are typically buried at depths of 0.5 to 1.0 meters (Allred and Redman, 2010). Based on the results of this study, which was conducted over very poorly drained to well drained, moderately-fine and fine textured soils in western Ohio, these depths can be successfully imaged with GPR using a lower frequency (200 MHz) antenna.

2. All radar records required processing to remove low frequency noise and improve signal amplification. These processing procedures are necessary to enhance the signal to noise ratio and improve the interpretability of buried agricultural drainage pipes. However, even after processing, some pipes were masked by high levels of background noise and not evident on radar records.

3. The interpretative quality of GPR data was lessened by features in the soil that produce similar GPR responses, the presence of crop residue and highly irregular soil surfaces caused by tillage operations. These features and properties caused unwanted noise and produced uncertainty in the identification and location of drainage pipes. Different adaptive field procedures are needed to traverse fields with different amounts of residue and surface roughness, and produce radar images with minimal background noise and high signal to noise ratios.

4. Temporal differences in soil moisture affect the detectability of drainage pipes. In Ohio, previous research by Allred et al. (2005) indicated that the detection of buried agricultural drainage pipes with GPR is more likely under drained, dry to moderately wet soil conditions than under extremely wet soil conditions. At the time of this investigation, soils were moist, water tables were high, and water was observed in pipes that had been purposely broken. These conditions are not optimal for the detection of drainage pipes with GPR. Returning to these sites during a drier time of the year may provide more acceptable results.

5. The use of systematic grid surveys and 3D-GPR imaging resulted in improved clarity, positioning, and confirmation of buried agricultural drainage pipes than random transects. However, grid methods are more time-consuming than random GPR transects. During field investigations, an experienced tile-probe operator proved faster and more efficient than GPR in detecting agricultural drainage pipes and mapping there alignments.

6. This study provided an opportunity for soil scientists in Ohio to view and operate an EMI meter. The resulting EC_a data and maps demonstrate the use of EMI to identify soil and management zones, map soil inclusions, and predict differences in soils and soil properties. At the two study sites surveyed with EMI, differences in EC_a were associated with spatial changes in one or more soil physiochemical properties.

It was the pleasure of Jim Doolittle and the National Soil Survey Center to be of assistance to you and your fine staff.

DAVID R. HOOVER
Acting Director
National Soil Survey Center

Attachment (Technical Report)

cc:
Steve Baker, State Soil Scientist, NRCS, Columbus, OH
Travis Neely, Soil Survey Regional Director, Region 11, NRCS, Indianapolis, IN
LaRae Baker, Soil Conservationist, NRCS, Bellefontaine, OH
Chris Davis, Soil Scientist, NRCS, Findlay, OH,
Jeff Glanville, Soil Scientist/Soil Database Manager, NRCS, Columbus, OH
Charles Hanner, Soil Scientist, NRCS, Findlay, OH
Melissa Hanner, Soil Scientist, NRCS, Tiffin, OH
Neil Martin, Soil Scientist, NRCS, Findlay, OH,
Donald McClure, Soil Scientist, NRCS, Findlay, OH
Chad Meenach, Civil Engineering Technician, NRCS, Marion, OH
David Smith, Director, Soil Science Division, NRCS, Washington, DC
Jim Doolittle, Research Soil Scientist, Soil Survey Research & Laboratory, NSSC, NRCS, Newtown Square, PA
Paul Finnell, Soil Scientist, NSSC Region 11 Liaison, NSSC, MS 35, NRCS, Lincoln, NE
J. Cameron Loerch, Acting National Leader, Soil Survey Research & Laboratory, NSSC, MS 41, NRCS, Lincoln, NE
John (Wes) Tuttle, Soil Scientist, Soil Survey Research & Laboratory, NSSC, NRCS, Wilkesboro, NC

Geophysical Investigation in western Ohio, May 14 to 16, 2013

Jim Doolittle

Ground-Penetrating Radar (GPR) Investigation of Buried Agricultural Drainage Pipes:
In the Midwest, an extensive system of subsurface pipes and ditches has been installed to drain wetlands for farming. These pipes are very effective and have brought additional acreages into cultivation and helped to increase yields. However, some drained, former wetlands remain marginally suited to farming because of inadequate soil water drainage. Many of these wetlands are being restored through initiatives such as the Wetlands Reserve Program. The restoration of wetlands benefits biodiversity, improves water quality, and provides basins for the temporary retention of flood waters. The restoration of former wetlands requires knowledge of the number, location, and alignment of all buried drainage pipes. Once located, these drainage pipes can be removed or plugged to restore the wetlands.

Drainage pipes are used to lower the water table. The most common drainage pipe is 10-cm in diameter and constructed of either clay tile (prior to the 1960s) or more recently, corrugated plastic tubing (Allred et al., 2004). In agricultural fields, it is not uncommon to have multiple generations of drainage pipes (Roger et al., 2005). To increase drainage efficiency and/or to replace damaged or impaired (clogged with sediment or damaged) pipes, a new system of pipes is often installed without removing the older system (Roger et al., 2005). Maps and records documenting the locations of drainage pipes are seldom kept and little knowledge is often available on previously installed systems.

Figure 1. Shovels, augers, and tiling probes are commonly used by NRCS in Ohio to located buried agricultural drainage pipes.

To locate buried drainage pipes, a tile-probe rod is commonly used (Figure 1). This method is slow, costly, and labor intensive, and cannot assure that all pipes have been identified. Alternative, more expedient and efficient methods for locating buried agricultural drainage pipes are needed. Geophysical

methods are being increasingly used in agriculture and for the detection of drainage pipes. Allred et al. (2004) provides an excellent review of the use of electromagnetic induction (EMI), geomagnetic surveying, ground-penetrating radar (GPR), and resistivity for the detection of buried drainage pipes in Ohio. Of these four near-surface geophysical methods, GPR proved the most capable of detecting buried agricultural drainage pipes.

Chow and Rees (1989) were among the first to discuss the use of GPR for the detection of subsurface drainage pipes. These researchers noted that when traversed orthogonally to their long axis with a radar antenna; buried drainage pipes produce distinct hyperbolic patterns on radar records. However, rock fragments, larger roots, animal burrows, soil and moisture discontinuities can produce similar hyperbolic patterns, which complicate interpretations (Chow and Rees, 1989). When GPR traverse lines are conducted parallel to their long axis, buried drainage pipes produce banded planar features, which can be confused with soil interfaces on radar records.

The size and depth of a drainage pipe affects detection. Large, shallowly buried pipes are more easily detected than smaller, more deeply buried pipes. However, the type of drainage pipe present, whether clay or corrugated plastic tubing, does not appear to have a significant effect on detection (Allred and Daniels, 2008).

Drainage pipes are usually installed in the more poorly drained areas of fields, which have soils with higher moisture and often clay contents. High soil moisture and clay contents adversely affect the use of GPR by increasing the rate of signal attenuation, limiting the depth of penetration, and reducing the resolution of subsurface interfaces.

In many fields, the number, orientation and depth of buried drainage pipes are unknown and these features can be easily missed or misinterpreted on two-dimensional (2D) radar records. The identification of buried drainage systems requires more than randomly conducted radar traverses across fields. More time-consuming and labor-intensive systematic grid surveys and the creation of three-dimension (3D) pseudo-images of the subsurface are required for the acceptable identification of drainage pipes. Allred et al. (2004b) observed that 3D-GPR grid surveys offer the best chance for finding buried drainage pipes. Allred and Redman (2010) and Allred et al. (2003) found that for grid surveys, 1.2 to 1.5 m spacing between traverse lines is acceptable for the detection of drainage pipes. Using 3D-GPR, Allred and Redman (2010), working in a restricted area over known drainage pipes, were able to identify known obstructions and assess the structural integrity and water conveyance properties of drainage pipes. However, to assess the structural integrity and water conveyance functionality of drainage pipes, a larger number of more closely spaced traverses are required, making this method impractical for many studies.

Allred et al. (2004) used 3D-GPR grid surveys to effectively identify and trace the alignment of buried agricultural drainage pipes at 11 research sites in Ohio. In that study, systematic GPR grid surveys had an averaged effectiveness of 81 % in detecting known drainage pipes buried at depths of 0.5 to 1.0 m in soils with different textures (sandy loam to clay). However, the effectiveness of GPR in detecting buried pipes varied from 0 to 100% among the eleven sites depending on hydropedological conditions. In expanded studies covering fourteen sites, which ranged in size from 200 to12000 m^2, Allred et al. (2005) and Allred and Daniels (2008) reported a reduced averaged effectiveness of 74%. Based on these studies, it was concluded that GPR is reasonably effective in finding clay tile and corrugated plastic tubing drainage pipes down to depths of about 1 meter in most Ohio soils (Allred and Redman, 2010).

Allred et al. (2005) noted that the effectiveness of GPR for drainage pipe detection requires not only the use of systematic grid surveying methods, but "careful consideration of computer processing procedures, equipment parameters, site conditions, and field operations." In the studies conducted by Allred and others, the use of advanced computer processing procedures was considered essential for the

identification of buried pipes. In many soils, without significant processing, neither 2D radar record nor 3D-GPR amplitude maps provide sufficient clues to identify buried drainage pipe systems.

The effects of shallow hydrology, soil texture, drainage pipe orientation, drainage pipe size and depth, and survey procedures on the effectiveness of GPR are summarized in Allred et al. (2003, 2005) and Allred and Daniels (2008). Allred et al. (2005) observed that drained, moderately wet conditions are better suited to mapping drainage pipes with GPR than undrained extremely wet conditions. In addition, field conditions are considered more favorable when soils are moderately dry, the water table is located below the drainage pipes, and the drainage pipe is air-filled. The worst soil condition for detecting drainage pipes with GPR occurs when the water table is above the level of the drainage pipes and the pipes are water- and/or sediment-filled (Allred et al., 2003).

The present study explores the potential of using GPR to effectively and expediently detect drainage pipes in very poorly drained to well drained, moderately-fine and fine textured soils formed in the tills of western Ohio (Champaign, Darke, and Logan Counties). This study evaluated the impacts of soil texture, hydrology, and surface conditions on the detection of buried agricultural drainage pipes constructed of different materials, having different diameters and orientations, and buried at different depths.

Figure 2. Collecting GPR data with a SIR-3000 system, 200 MHz antenna, survey wheel, and GPS.

Equipment:

The radar unit is the TerraSIRch Subsurface Interface Radar (SIR) System-3000 (here after referred to as the SIR-3000), manufactured by Geophysical Survey Systems, Inc. (GSSI; Salem, NH).[1] The SIR-3000 consists of a digital control unit (DC-3000) with keypad, SVGA video screen, and connector panel. A 10.8-volt lithium-ion rechargeable battery powers the system. The SIR-3000 weighs about 4.1 kg (9 lbs) and is backpack portable (Figure 2). With an antenna, the SIR-3000 requires two people to operate. Jol (2009) and Daniels (2004) discuss the use and operation of GPR. A 200 MHz antenna was used in this

[1] Manufacturer's names are provided for specific information; use does not constitute endorsement.

investigation (Figure 2). In a comparative study in Ohio, using 100, 250 and 500 MHz antennas, Allred et al. (2003) observed that the 250 MHz antenna provided the best imagery of buried drainage pipes.

The RADAN for Windows (version 7.0) software program (developed by GSSI) was used to process the radar records.[1] Processing included: header editing, setting the initial pulse to time zero, color table and transformation selection, signal stacking, horizontal high pass filtration, and range gain adjustments (refer to Jol (2009) and Daniels (2004) for discussions of these techniques).

The SIR-3000 system contains a setup for the use of a GPS receiver with a serial data recorder (SDR). With this setup, each scan of the radar can be georeferenced (position/time matched). Following data collection, a subprogram within the RADAN for Windows is used to proportionally adjust the position of each radar scan according to the time stamp of the two nearest positions recorded with the GPS receiver. A Trimble AgGPS114 L-band DGPS (differential GPS) antenna (Trimble, Sunnyvale, CA) was used to collect position data (Figure 2).[1] Position data were recorded at a rate of one reading per second. The scanning rate of the GPR was 64 scans per second. The scanning time varied with site conditions and ranged from 40 to 60 ns (nanoseconds).

Calibration of GPR:

Ground-penetrating radar is a time scaled system. The system measures the time that it takes electromagnetic energy to travel from an antenna to an interface (e.g., soil horizon, buried pipe) and back. To convert the travel time into a depth scale, either the velocity of pulse propagation or the depth to a reflector must be known. The relationships among depth (D), two-way pulse travel time (T), and velocity of propagation (v) are described in equation [1] (after Daniels, 2004):

$$v = 2D/T \qquad [1]$$

The velocity of propagation is principally affected by the relative dielectric permittivity (E_r) of the profiled material(s) according to equation [2] (after Daniels, 2004):

$$E_r = (C/v)^2 \qquad [2]$$

In equation [2], C is the velocity of light in a vacuum (0.3 m/ns). In soils, the amount and physical state (temperature dependent) of water have the greatest affect on the E_r and v. Dielectric permittivity ranges from 1 for air, to 78 to 88 for water (Cassidy, 2009). Small increments in soil moisture result in substantial increases in the relative permittivity of soils (Daniels, 2004). Using a 100 MHz antenna, Daniels (2004) observed that the relative dielectric permittivity of most dry mineral soil materials is between 2 and 10, while for most wet mineral soil materials, it is between 10 and 30.

Based on the measured depths to a shallowly buried (< 50 cm) metal plate and using equations [1] and [2], the estimated averaged v and E_r were: 0.0683 m/ns and 19.3 in an area of Brookston soils (Champaign County), 0.0724 m/ns and 17.2 in an area of Westland (Darke County), and 0.05935 m/ns and 25.5 in an area of Blount (Logan County). These values are comparable to those obtained by Allred and Redman (2010) in an area of Crosby soils under drained, moderately wet conditions in Franklin County (v was 0.0675 m/ns and the E_r was 19.7). Spatial and depth variability in v and E_r will affect accuracy of all soil depth measurements.

The amount of energy reflected back to an antenna is a function of the dielectric gradient that exists across a soil interface or boundary. The greater and/or more abrupt the contrast in the dielectric properties of the adjoining materials, the greater the amount of energy reflected back to the antenna, and the higher the amplitude of the reflected signal appearing on radar records. Soil horizons and features that

have similar dielectric properties are poor reflectors of electromagnetic energy and are often difficult to identify on radar records. The reflection coefficient, R, is used to express the difference in relative dielectric permittivity that exists between two adjoining materials. The reflection coefficient is proportional to the strength of reflected signal and is expressed as (Davis and Annan, 1989):

$$R = \frac{\sqrt{Er_1} - \sqrt{Er_2}}{\sqrt{Er_1} + \sqrt{Er_2}} \qquad [3]$$

In equation [3], E_{r1} is the dielectric permittivity of the upper layer, and Er_2 is the permittivity of the lower layer. The E_r of soil materials is strongly dependent upon moisture content. As a consequence, the amount of energy reflected back to the radar's antenna is greatly influenced by the abruptness and difference in moisture contents that exist between soil horizons, layers or features. The strength of the radar response from buried drainage pipes is dependent upon the contrast in dielectric permittivity that exists between the encompassing soil matrix and the material within the pipe (air, water, and/or sediment). Because of the abrupt boundary and the contrast in dielectric permittivity, an air filled pipe surrounded by a saturated soil matrix provides a very strong radar response. However, a saturated sediment or water-filled pipe surrounded by a saturated soil matrix will provide a weak radar response. Because of changes in soils, soil properties, topography, and drainage pipe depth and condition, the GPR response from a given pipe will vary spatially across the field.

Study Sites:

Study Site 1 (40.2605 N latitude, 83.8096 W longitude) is located in a cultivated field about 4.6 km west-northwest of West Liberty in Champaign County. The site is mapped as Brookston silty clay loam, 0 to 2 % slopes (BsA), Miami silt loam, 2 to 6 % slopes (MiB), and Miamian silt loam, 2 to 6 % slopes (MnB) (Figure 3). The very deep, poorly drained Brookston, moderately well drained Miami, and well drained Miamian soils formed in loess or silty materials and an underlying loamy till on till plains and moraines. The taxonomic classifications of the named soils at this and the other four study sites are listed in Table 1.

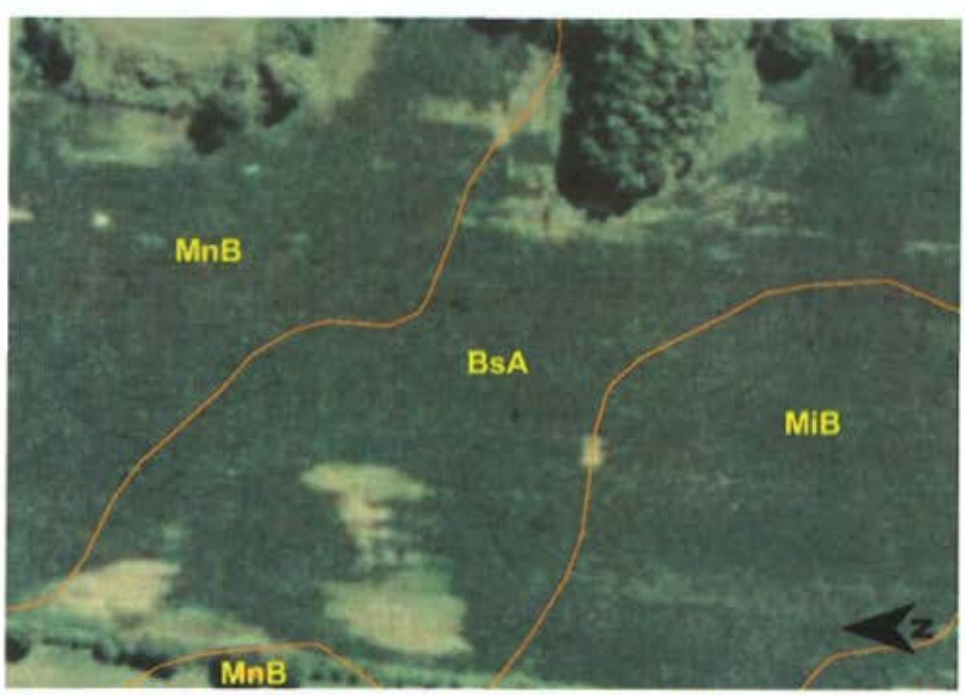

Figure 3. Soil map of Study Site 1, which is located in Champaign County.

Table 1. Taxonomic classification of the soils recognized at the study sites.

Soil Series	Taxonomic Classification
Blount	Fine, illitic, mesic Aeric Epiaqualfs
Brookston	Fine-loamy, mixed, superactive, mesic Typic Argiaquolls
Carlisle	Euic mesic Typic Haplosaprists
Edwards	Marly, euic, mesic Limnic Haplosaprists
Eldean	Fine, mixed, superactive, mesic Typic Hapludalfs
Miami	Fine-loamy, mixed, active, mesic Oxyaquic Hapludalfs
Miamian	Fine, mixed, active, mesic Oxyaquic Hapludalfs
Patton	Fine-silty, mixed, superactive, mesic Typic Endoaquolls
Westland	Fine-loamy, mixed, superactive, mesic Typic Argiaquolls

Study Site 2 (40.0292 N latitude, 84.7323 W longitude) is located in a cultivated field about 2.4 km southeast of Palestine in Darke County. The site is mapped as Westland silty clay loam (Ws), Eldean-Miamian complex, 6 to 12 % slopes, eroded (ErC2), and Patton silty clay loam (Pa) (Figure 4). The poorly drained and very poorly drained Westland soils are deep to calcareous, stratified gravelly and sandy outwash. Westland soils are capped with as much as 51 cm of loess or silty materials. The well drained Eldean soils are moderately deep to calcareous sandy and gravelly material. Eldean soils formed in outwash materials on outwash terraces, kames, and moraines. In some places, the upper part of the Eldean solum formed in silty or loamy alluvium or in loess as much as 46 cm. The very deep, poorly drained and very poorly drained Patton soils formed in glaciolacustrine deposits on stream terraces and glacial lake plains. The taxonomic classifications of these soils are listed in Table 1.

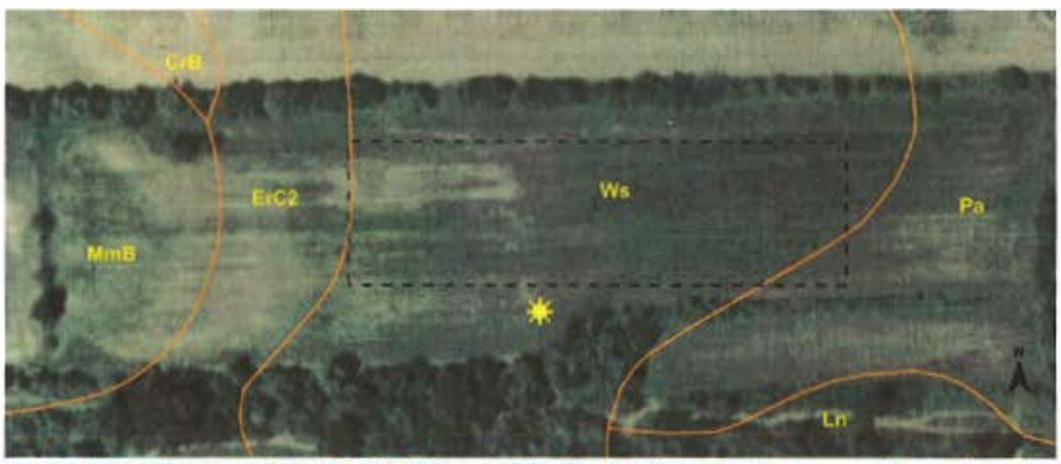

Figure 4. In this soil map of Study Site 2 located in Darke County, the approximate location of the GPR traverse is identified by a spot symbol. The approximate area surveyed with the EMI meter is enclosed by black-colored segmented lines.

Study Site 3 (40.0543 N latitude, 84.6128 W longitude) is located in a cultivated field about 5.7 km south-southeast of Greenville in Darke County. The site selected for GPR survey is mapped as Patton silty clay (Pa) and Carlisle muck (Ca). The site selected for EMI survey is located to the south in an area mapped as Brookston silty clay loam (Br), Miamian clay loam, 6 to 12% slopes, severely eroded (MmC3), and Miamian silt loam, 2 to 6% slopes (MmB). The very deep, very poorly drained Carlisle soils formed in woody and herbaceous organic materials in depressions. Figure 5 is a soil map of Study Site 3. On this map, the locations of the GPR traverse line and the area surveyed with EMI have been identified with a spot symbol and enclosed in black, segmented lines, respectively. The taxonomic classifications of the soils are listed in Table 1.

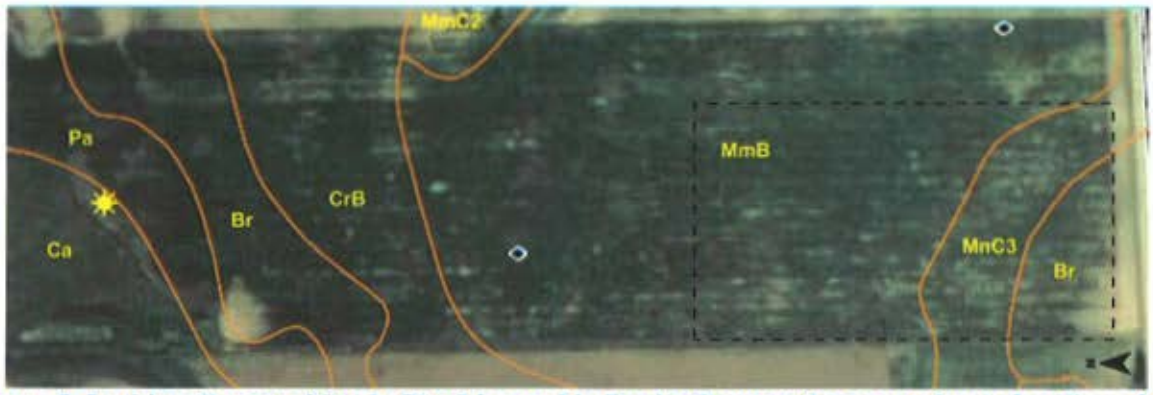

Figure 5. In this soil map of Study Site 3 located in Darke County, the approximate location of the GPR traverse is identified by a spot symbol. The approximate area surveyed with the EMI meter is enclosed by black colored segmented lines.

Study Site 4 (40.3614 N latitude, 83.8877 W longitude) is located in a cultivated field about 5.8 km north-northeast of De Graff in Logan County. The site selected for the GPR grid survey is mapped Blount silt loam, 0 to 2 % slopes (BoA) and Edwards muck (Ed). The somewhat poorly drained Blount soils are moderately deep or deep to dense till. Blount soils formed in till on till plains. The very deep, very poorly drained Edwards soils formed in herbaceous organic materials, which are 61 to 130 cm thick, overlying marly materials in depressions. The approximate location of Study Site 4 is shown in Figure 6. On this map, the soil line separating the Blount and Edwards delineations is out-of-place in the area of the GPR survey grid. The survey was conducted solely in the area of Blount silt loam, 0 to 2 % slopes. The taxonomic classifications of these soils are listed in Table 1.

Figure 6. In this soil map of Study Site 4 located in Logan County, the approximate location of the GPR grid is identified by the yellow-colored square.

Survey Procedures:
Multiple GPR traverses were completed across each site by pulling the 200 MHz antenna along the ground surface (Figures 2 and 7). A survey wheel was attached to the antenna (Figure 7). An integrated odometer on the survey wheel measured distance along each traverse line. Each radar traverse was stored as a separate file. All radar records were similarly processed to improve signal positioning, remove low and high frequency noise, and enhance signal amplification.

Figure 7. Buried drainage pipes are located by pulling the 200 MHz antenna (with a survey wheel attached) across a suspected area.

Buried agricultural drains can be detected on 2D radar records, but verification requires multiple passes over a buried pipe with an antenna. As noted by Allred et al. (2005, 2008) and Allred and Redman (2010), the successful detection and identification of buried drainage pipes requires the use of grid survey procedures, the creation of 3D-pseudo-images, and the use of amplitude-slice methods. Three-dimensional GPR and amplitude-slice methods allow the visualization of data volumes from different perspectives and cross-sections (Beres et al., 1999). This methodology assists the detection, outlines the structure and alignment, and improves the interpretation of drainage pipes. Three-dimensional GPR results in more comprehensive and less ambiguous interpretations than traditional 2D-GPR interpretations. However, the acquisition of 3D-GPR data requires greater expenditures of time and labor and is more computationally demanding than 2D radar modeling and interpretations (Allred and Redman, 2010).

To construct a 3D pseudo-image of the subsurface, a relatively small area is intensively surveyed with a series of closely-spaced, parallel GPR traverse lines. A relatively dense set of grid lines is necessary to resolve the geometry and size of different subsurface features and to prevent spatially aliasing the data (Grasmueck and Green, 1996). Allred and Redman (2010) observed that spacings of 1.2 to 1.5 m are

adequate to image drainage lines. Conducting two sets of multiple GPR traverse lines in orthogonal directions across small grid areas helps to insure the detection of drainage pipes whose orientation is unknown, but adds greatly to the expenditure of resources. Lehmann and Green (1999) discuss considerations that are important for the completion of 3D-GPR surveys.

Results:

On most "raw" or unprocessed radar records, which could be reviewed in the field, drainage pipes were faint or unobservable because of high levels of background noise and weak or low amplitude reflections from the pipes themselves. Low amplitude reflections are attributed to saturated or moist soil conditions, lack of contrast between water- and/or sediment-filled pipes and the surrounding moist soils, and high rates of signal attenuation. At most of the sites, buried agricultural drainage pipes were detected on processed radar records. Processing required additional time and the processed radar records were not available for review in the field.

Figure 8 is a portion of a 2D radar record from Study Site 1 in Champaign County. On this radar record the horizontal and vertical scales are expressed in meters. Drainage pipes that are crossed at an angle with a GPR antenna will appear on radar records as inverted U- or V-shaped features commonly referred to as *reflection hyperbolas* by geophysicists. The apex of the hyperbola provides information on drainage pipe location and depth along the radar traverse line. On the radar record shown in Figure 8, a white-colored arrow identifies a confirmed drainage pipe that is buried at a depth of 30.5 cm. Other reflection hyperbolas are evident on this radar record. A confirmed rock fragment (at a depth of about 28 cm) produced the reflection hyperbola to the left of the red-colored arrow in Figure 5. Rock fragments are common in the tills of western Ohio and produce similar reflection hyperbolas as drainage pipes, increasing the complexity of analyses and causing some incorrect interpretations. Ground-truth auger borings are required to confirm the identity of point reflectors detected on 2D radar records.

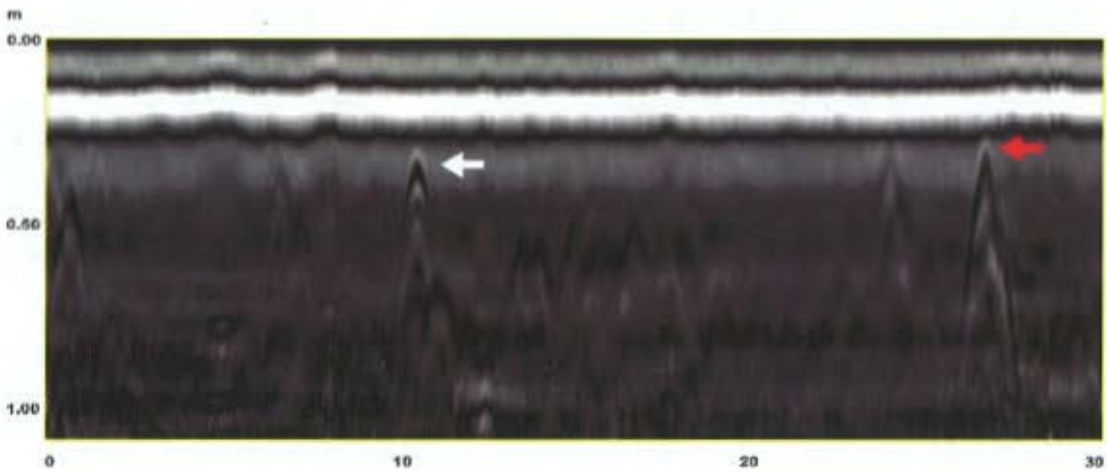

Figure 8. Reflection hyperbolas identify point objects buried in an area of Brookston soils at Study Site 1. Colored arrows indicate a confirmed drainage pipe (white) and a large rock fragment (red).

The composition of the materials used in drainage pipes (clay tile or corrugated plastic tubing) is known to have little impact on the GPR response (Allred and Redman et al., 2010). The response from a buried drainage pipe is principally controlled by the contrast in relative dielectric permittivity between the material contained within the pipe (air, water, and/or soil) and the surrounding soil matrix (Zeng and McMechan, 1997). As a consequence, an air-filled pipe will have a stronger response than a water- or sediment-filled pipe (Allred and Redman, 2010). At the time of this investigation, soils were moist, water

tables were high, and water was observed in pipes that had been purposely broken. These conditions are not the most favorable for the detection of drainage pipes with GPR. Returning to these sites during a drier time of the year may provide more acceptable results.

Figure 9 is a 3D display of a georeferenced 2D radar record collected at Study Site 1. On this 3D display, the vertical scale is expressed in meters; the spatial scale is expressed in the Universal Transverse Mercator (UTM) geographic coordinate system. In this example, the radar antenna was pulled in a serpentine pattern over a known drainage pipe. In Figure 9, white arrows identify reflection hyperbolas produced by the buried pipe and a yellow, segmented line has been used to indicate the trend and orientation of the buried line. The depth to this pipe ranges from 46 to 50 cm. The use of 3D-GPR can help to verify the identity of buried point anomalies (a series of point reflectors detected at a similar depth and arranged in a linear pattern provide strong evidence supporting the presence of a buried pipe) and provides information on the geometry of drainage systems.

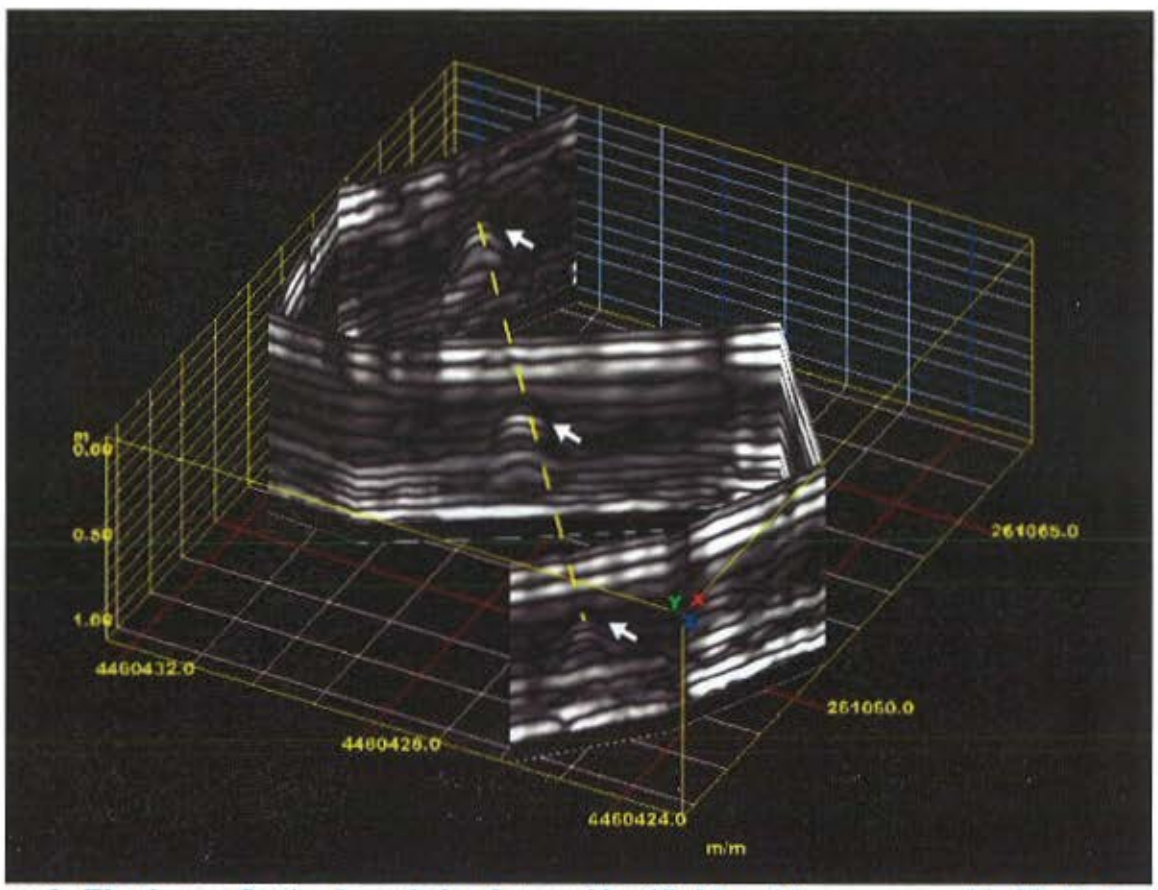

Figure 9. The three reflection hyperbolas that are identified by white arrows on this 3D display of a radar record are from a buried drainage pipe that was crossed in a serpentine pattern with the 200 MHz antenna. The radar record was collected in an area of Brookston soils at Study Site 1.

Figure 10 is a 2D radar record from an area of Westland soil at Study Site 2 in Darke County. On this 2D radar record, the vertical scale is expressed in meters and the horizontal scale is expressed in degrees of longitude and latitude. In Figure 10, a faint reflection hyperbola that is believed to be a drainage pipe has been identified with a yellow arrow. This feature is so weakly expressed that it was not identified in the field. Unfavorable soil conditions (high water table; moist to saturated, moderately-fine to fine textured soil materials; sediment- or water-filled drainage pipes) provide possible explanations for the weak reflections

from this suspected buried pipe. The moderate clay (averages 24 to 35 percent clay) and moisture contents of the Westland soil causes moderately-high signal attenuation rates that limit penetration and makes this soil poorly suited to GPR soil investigations. In Westland soils, the depth to stratified gravelly and sandy outwash ranges from about 75 to 155 cm. If abrupt, the interface separating the loamy sediments from the underlying outwash should provide a highly contrasting boundary and produce a strong radar reflection. However, signal attenuation was too severe, depth of signal penetration too limited, and the signal to noise ratio so low that this interface could not be clearly imaged with the GPR under the existing field conditions.

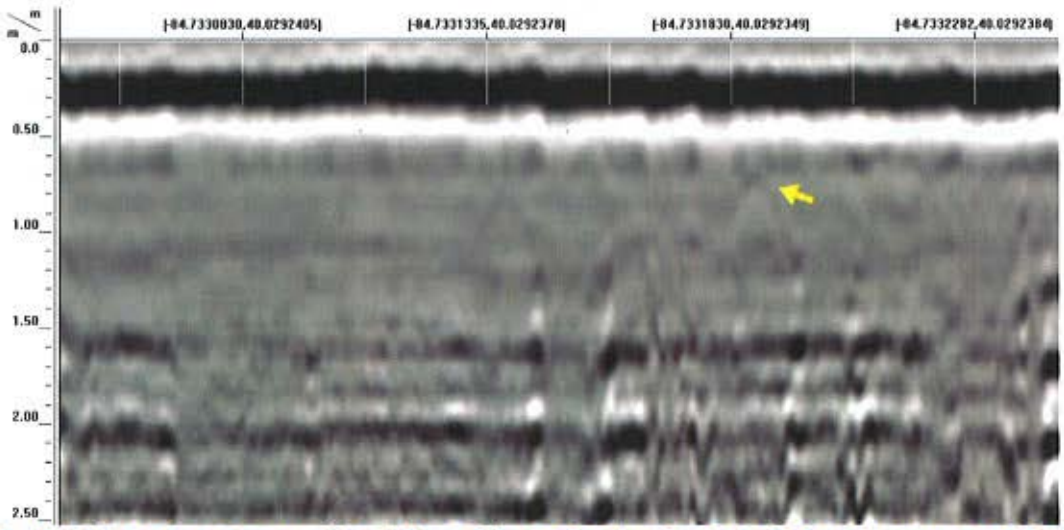

Figure 10. A white-colored arrow identifies a faint reflection hyperbola from a suspected drainage pipe on this radar record from an area of Westland soil at Study Site 2 in Darke County.

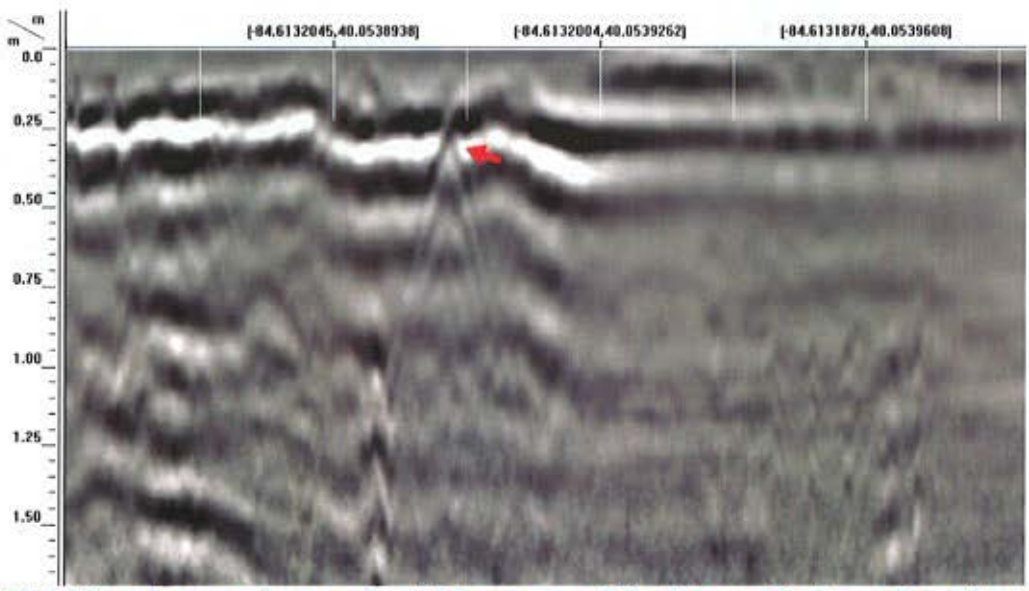

Figure 11. This 2D radar record was collected in an area of Carlisle and Patton soils at Study Site 3 in Darke County. The arrow points to a reflection hyperbola believed to be a drainage pipe.

Figure 11 is a 2D radar record from an area of Carlisle and Patton soils at Study Site 3 in Darke County. On this 2D radar record, the vertical scale is expressed in meters and the horizontal scale is expressed in degrees of longitude and latitude. On this radar record, a reflection hyperbola that could be a drainage pipe has been

identified with a red arrow. However, other reflection hyperbolas are evident on this radar record. Some of these hyperbolas are caused by jarring or lifting the antenna off of the ground surface. Other reflection hyperbolas are the result of point reflectors buried in the soil. These examples demonstrate the difficulty experienced in identifying buried drainage pipes on radar records. In Figure 11, a near-surface, planar reflector undergoes a noticeable change in amplitude and expression to the right of the identified reflection hyperbola (red arrow). This change in expression is caused by changes in soil physical properties. An increase rate of signal attenuation, which is caused by increase in water and clay contents, is offered as a possible explanation for the weaker reflections in the right-hand portion of this radar record.

As noted by Allred et al. (2005, 2008) and Allred and Redman (2010), the use of grid survey methods, the creation of 3D-pseudo-images, and the use of amplitude-slice displays are needed to acceptably identify buried drainage pipes. Figure 12 contains two 3D-GPR pseudo-images of a small grid site (Study Site 4) in Logan County. In Figure 12, the pseudo-image on the left is a solid cube; the pseudo-image on the right has a 19.0 by 14.0 by 0.7 m inset cube graphically removed to reveal two drainage pipes along its base. In order to construct these 3D pseudo-images, GPR data were collected along a series of 16 traverse lines that were parallel with the x-axis (left-foreground). These traverse lines were 20 m long and spaced 1 m apart. These procedures produced a 20 by 15m (300 m^2) grid. Data from the 16, 2D (x, z) radar records were later gridded and interpolated in the y-direction, and the data presented as 3D pseudo-images (Figure 12). Because data were continuously recorded along the x-axis (left-foreground), greater detail is evident along this axis of the pseudo-images than along the y-axis (right-foreground) where data were collected at 100 cm intervals (traverse line spacing). Data shown along the y-axis are spatially aliased, notably "smeared", and more poorly represented.

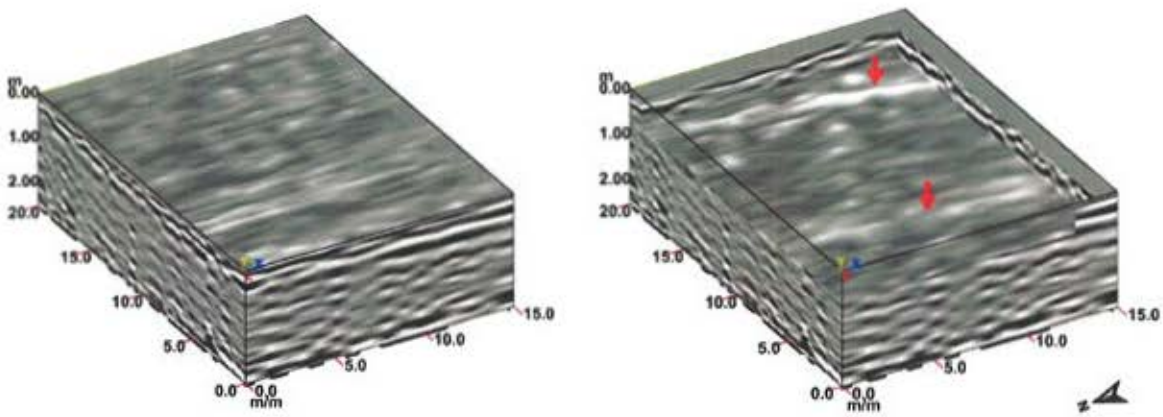

Figure 12. These 3D pseudo-images are from a drained area of Blount soils in Logan County. A solid 3D cube of the grid site is shown on the left; a cube with the upper 70 cm of the soil profile removed is shown on the right. The two, high amplitude (colored white), linear reflector (identified by red arrows) in the right-hand pseudo-image represent buried drainage pipes.

Along the sidewalls of the pseudo-images shown in Figure 12, high amplitude planar reflections are evident at depths ranging from 10 to 35 cm. These reflections are believed to represent the interface separating the surface layers (Ap and A horizons) from the Bt horizon of the Blount soil. Along the base of the inset cube, the two linear, high-amplitude (colored white) linear reflection patterns (identified by red arrows) are the result of buried drainage pipes. These features were not recognized on the 2D radar

records during a cursory review of the data in the field. The reflection pattern from the pipe that is located further to the east (uppermost pattern) is higher in amplitude and better defined. As this pipe is located further from the delineation of very poorly drained Edwards soil, is slightly higher-lying and presumably better drained, its higher amplitude could be the result of radar signals reflecting off an air-filled pipe surrounded by moist soil materials. The pipe located nearer the lower margin of the grid, is located in a slightly lower-lying and presumably more imperfectly drained area. The lower amplitude of this feature could be the result of radar signals reflecting off a water-filled pipe surround by moist or saturated soil materials. In this case, the reflection coefficient would be lower than in the first case and the pipe world be more poorly imaged with GPR.

High-Intensity Soil Surveys using Electromagnetic Induction (EMI:
Alternative methods for mapping and examining soils and soil properties are being evaluated by the USDA-NRCS. Electromagnetic induction meters are being increasingly used by soil scientists for high intensity soil surveys, site assessments, and site-specific management projects. This geophysical method has significant advantages over conventional soil survey techniques because of its speed and ease of use. In Illinois, Doolittle et al. (2008) used EMI maps to identify and delineate soil polygons and to help improve the quality of a high-intensity (order one) soil survey. The information provided by EC_a maps and additional soil sampling lead soil scientists to reevaluate soil mapping decisions and conceptual soil-landscape models, recognize different soils, and refine soil maps. A significant impact of the use of EMI data was the increased confidence of soil scientists in their mapping decisions (Doolittle et al., 2008). The use of EMI, if available, is recommended for high intensity soil surveys (Doolittle et al., 2008).

Electromagnetic induction methods involve the use of instruments known as ground conductivity meters (GCM). A GCM consists of a transmitter coil and either one or two receiver coil(s) spaced at a set distance(s) apart. Ground conductivity meters operate by generating an alternating electrical current, which is passed through the transmitter coil. This alternating electrical current generates a time-varying electromagnetic field above the surface; the primary electromagnetic field. The primary electromagnetic field induces eddy currents to flow in the soil. These currents generate a secondary electromagnetic field, which propagates through the ground. The secondary field is proportional to the ground current and is used to calculate the soil's "apparent" or "bulk" electrical conductivity. The amplitude and phase components of these two electromagnetic fields are measured by the receiver coil(s).

Apparent electrical conductivity (EC_a) is a weighted, average measurement for a column of earthen materials to a specific depth (Greenhouse and Slaine, 1983). Apparent conductivity is a measure of the soil's ability to conduct electrical currents. Variations in EC_a are produced by changes in the electrical conductivity of earthen materials. The electrical conductivity of soils is influenced by the type and concentration of ions in solution, the amount and type of clays in the soil matrix, the volumetric water content, and the temperature and phase of the soil water (McNeill, 1980). The EC_a of soils will increase with increases in soluble salts, water, and/or clay contents (Kachanoski et al., 1988; Rhoades et al., 1976). In many areas, patterns of EC_a corresponded well with the soil patterns shown on soil survey maps (Jaynes, 1995). Because of the larger number of observations, maps of apparent conductivity provide higher levels of resolution than soil maps prepared with conventional methods (Jaynes, 1995).

Considerable research has been conducted into understanding the soil properties that influence EC_a. Even though interpretations can be complicated by the interaction of multiple soil properties, EC_a has been used to infer and map variations in soils and soil properties at different spatial scales and levels of resolution. Variations in EC_a have been associated with changes in particle size distribution, clay mineralogy, bulk density, CEC, salinity, plant nutrients, and organic and moisture contents. Presently, EC_a mapping is recognized as one of the most valuable methods in agriculture for measuring the spatial variability of soils and soil properties at field and landscape scales (Lück et al., 2009; Corwin, 2008).

Equipment:
The EM38-MK2 meter (Geonics Limited; Mississauga, Ontario) was used in this study.[2] Operating procedures for the EM38-MK2 meter are described by Geonics Limited (2007). The EM38-MK2 meter operates at a frequency of 14.5 kHz and weighs about 5.4 kg (11.9 lbs.). The EM38-MK2 provides measurement of both the quadrature phase (apparent conductivity) and in-phase (apparent magnetic susceptibility) components within two distinct depth ranges, all simultaneously, without any requirement for soil-to-instrument contact. The meter has one transmitter coil and two receiver coils, which are separated from the transmitter coil at distances of 1.0 and 0.5 m. This configuration provides two nominal exploration depths of 1.5 and 0.75 m when the meter is held in the vertical dipole orientation (VDO), and 0.75 and 0.375 m when the meter is held in the horizontal dipole orientation (HDO).

The Geonics DAS70 Data Acquisition System was used with the EM38-MK2 meter to record and store both EC_a and GPS data. The acquisition system consists of the EMI meter, an Allegro CX field computer (Juniper Systems, Logan, Utah), and a Trimble Ag114 L-band DGPS (differential GPS) antenna (Trimble, Sunnyvale, CA).[2] With the acquisition system, the meter is keypad operated and measurements are automatically triggered. The RTmap38MK2 software program developed by Geomar Software Inc. (Mississauga, Ontario) was used with the EM38-MK2 meter and the Allegro CX field computer to record, store, and process EC_a and GPS data.[2]

To help summarize the results of the EMI surveys, SURFER for Windows (version 10.0), developed by Golden Software, Inc. (Golden, CO), was used to construct the simulations shown in this report.[2] Grids of EC_a data were created using kriging methods with an octant search.

Figure 13. Soil scientists complete an EMI survey with an EM38-MK2 meter and an Allegro field computer.

Field Procedures:
Pedestrian surveys were completed with the EM38-MK2 meter across portions of the two sites located in Darke County. The EM38-MK2 meter was operated in the deeper-sensing, VDO. The instrument was

[2] Manufacturer's names are provided for specific information; use does not constitute endorsement.

operated in the continuous mode with measurements recorded at a rate of 1/sec. Where possible, the long axes of the meter was orientated parallel to the direction of traverse, and held about 5 cm above the ground surface (see Figure 13). Walking in a back and forth manner across each site along essentially parallel traverse lines, a total of 2676 and 5211 EC_a, measurements were recorded with the EM38-MK2 meter at Study Sites 2 and 3, respectively. At the time of the EMI surveys, soils were moist throughout. Apparent conductivity data were not temperature corrected to a standard temperature of 75° F.

Results:
Table 2 provides basic statistics for the EMI data that were collected at Study Site 2 in Darke County. In Table 2, the headings for the two columns represent the intercoil spacings of the transmitter and receiver coils. The theoretical exploration depths are 75 and 150 cm for the 50 and 100 cm intercoil spacings, respectively. In Table 2, with the exception of "Number", the unit of measure is mS/m. As evident in a comparison of the two depth measurements, the bulk averaged EC_a remains constant with depth.

Table 2. Apparent Conductivity Data collected with the EM38-MK2 in the Vertical Dipole Orientation at Study Site 2 in Darke County.

	EC_a - 50 cm	EC_a - 100 cm
Number	2676	2676
Minimum	5.0	15.2
25%-tile	29.4	26.8
75%-tile	41.2	44.0
Maximum	67.9	59.4
Average	35.4	35.6
Std. Dev.	7.6	9.4

For measurements obtained in the shallower-sensing, 50-cm intercoil spacing, EC_a ranged from about 5.0 to 67.9 mS/m. For the 50-cm intercoil spacing, one-half of the measurements were between about 29.4 and 41.2 mS/m. For the deeper-sensing 100-cm intercoil spacing, EC_a ranged from about 15.2 to 59.4 mS/m. One-half of these measurements were between about 26.8 and 44.0 mS/m. For the two exploration depths, the relatively narrow interquartile ranges suggest comparatively homogeneous soil conditions and properties across most of the survey area.

Figure 14 contains two plots of the EC_a data that were collected with the deeper-sensing, 100-cm intercoil spacing of the EM38-MK2 meter. The EC_a data are presented in 2D (upper plot) and 3D (lower plot) formats. Elevation data used to construct the 3D wireframe image were collected with the Trimble Ag114 L-band DGPS (differential GPS) antenna. The same color scales and ramps have been used in both plots. Soil boundary lines have been digitized from Web Soil Survey data[3].

In general, EC_a for the 0 to 150 cm depth interval increases towards the east and in a downslope direction. The increase in EC_a is attributed to presence of more saturated soil conditions and the presence of a higher water table in the lower-lying landscape positions. In addition, the higher EC_a may reflect higher bulk clay contents resulting from deeper depths to coarse-textured materials. As shown on the soil map in Figure 4, soils transition from Eldean-Miamian (ErC2) to Westland (Ws) to Patton (PA) along this slope gradient. The lower EC_a on the higher-lying, western portion of the study area is attributed to better soil drainage and the presence of stratified sandy and gravelly materials at moderately deep depths. The higher EC_a on the lower-lying eastern portion of the study area is attributed to the occurrence of poorly and very poorly drained, medium textured soils that are deep or very deep to stratified sandy and gravelly materials. However, as evident in Figure 14, this general spatial relationship is disrupted by more

[3] Soil Survey Staff, Natural Resources Conservation Service, United States Department of Agriculture. Web Soil Survey. Available online at http://websoilsurvey.nrcs.usda.gov/ accessed [05/23/2013].

intricate spatial EC_a patterns believed to represent inclusions of deeper or shallower to stratified sandy and gravelly material soils and soils with higher or lower bulk clay contents.

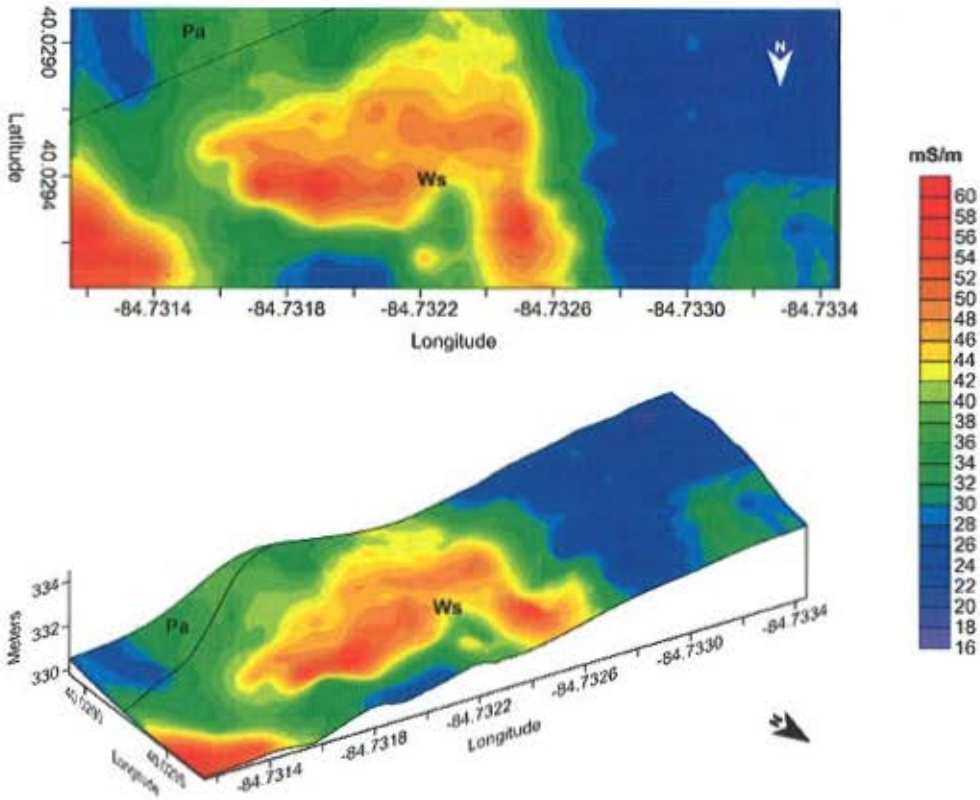

Figure 14. These 2D (upper) and 3D (lower) images show the spatial distribution of EC_a for the 0 to 150 cm depth interval across Study Site 2 in Darke County.

Table 3 provides basic statistics for the EMI data that were collected at Study Site 3 in Darke County. In Table 3, the headings for the two columns represent the intercoil spacings of the transmitter and receiver coils. The theoretical exploration depths are 75 and 150 cm for the 50 and 100 cm intercoil spacings, respectively. In Table 3, with the exception of "Number", the unit of measure is mS/m. As evident in this table, the bulk averaged EC_a remains constant with depth. However, compared with the data from Study Site 2 (Table 2), the soils at Study Site 3 have noticeably lower and less variable EC_a.

Table 3. Apparent Conductivity Data collected with the EM38-MK2 in the Vertical Dipole Orientation at Study Site 2 in Darke County.

	EC_a - 50 cm	EC_a - 100 cm
Number	5211	5211
Minimum	-26.7	-12.5
25%-tile	12.0	14.1
75%-tile	18.6	20.8
Maximum	35.3	33.0
Average	15.0	17.9
Std. Dev.	5.4	4.8

At Study Site 3, for measurements obtained in the deeper-sensing, 100-cm intercoil spacing, EC_a ranged from about -12.5 to 33.0 mS/m. Negative values are attributed to the presence of metallic artifact(s) scattered across the site. For the 100-cm intercoil spacing, one-half of the measurements were between about 14.1 and 20.8 mS/m. For the shallower-sensing 50-cm intercoil spacing, EC_a ranged from about -26.7 to 35.3 mS/m. One-half of these measurements were between about 12.0 and 18.6 mS/m. For the two exploration depths, the relatively narrow interquartile ranges suggest relatively homogeneous soil conditions and properties across most of the survey area.

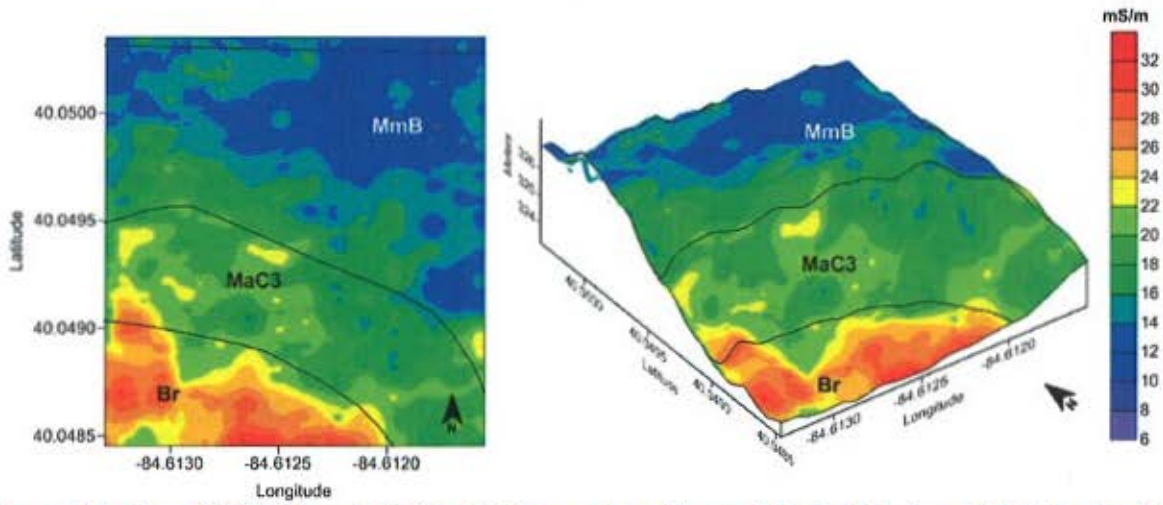

Figure 15. These 2D (left) and 3D (right) images show the spatial distribution of EC_a for the 0 to 150 cm depth interval across Study Site 3 in Darke County.

Figure 15 contain two plots of the EC_a data that were collected at Study Site 3 with the deeper-sensing, 100-cm intercoil spacing of the EM38-MK2 meter. The data are presented in 2D (left-hand plot) and 3D (right-hand plot) formats. Elevation data used to construct the 3D wireframe image were collected with the Trimble Ag114 L-band DGPS (differential GPS) antenna. The same color scales and ramps have been used in both plots. Soil boundary lines have been digitized from Web Soil Survey data[4].

In general, EC_a for the 0 to 150 cm depth interval increases towards the southwest and in a downslope direction. The increase in EC_a is attributed to presence of wetter soil conditions, higher water tables and perhaps higher clay contents. As shown on the soil map in Figure 5, soils transition in a downslope direction from Miamian (MmB and MmC3) to Brookston (Br). Both soils are very deep and formed in loess overlying loamy till. The lower EC_a on the higher-lying, northern portion of the study area is attributed to better soil drainage. The higher EC_a on the lower-lying, southwestern portion of the study area is attributed to presence of poorly drained Brookston soils. An area of intermediate EC_a conforms to a more sloping area mapped as an eroded phase of Miamian soils. The shallower depths to a clayey argillic horizon help to explain the intermediate EC_a that occurs within this delineation and landscape component.

This study has provided an opportunity for soil scientists in Ohio to view and operate an EMI meter. The resulting EC_a data and maps demonstrate the use of EMI to identify soil and management zones, and predict potential differences in soils, and soil properties. At the two study sites surveyed with EMI, differences in EC_a were associated with spatial changes in one or more soil physiochemical properties.

[4] Soil Survey Staff, Natural Resources Conservation Service, United States Department of Agriculture. Web Soil Survey. Available online at http://websoilsurvey.nrcs.usda.gov/ accessed [05/23/2013].

References:

Beres, M., P. Huggenberger, A.G. Green, and H. Horstmeyer, 1999. Using two- and three-dimensional georadar methods to characterize glaciofluvial architecture. *Sedimentary Geology* 129: 1-24.

Allred, B.J., and J.J. Daniels, 2008. Agricultural drainage pipe detection using ground-penetrating radar. In: *Handbook of Agricultural Geophysics*. Allred, B. J., J. J. Daniels, and M. Reza Ehsani (Eds). CRC Press; Boca Raton, Florida. pp. 363-374.

Allred, B.J., J.J. Daniels, N.R. Fausey, C. Chen, L. Peters, and H. Youn, 2005. Important considerations for locating buried agricultural drainage pipe using ground penetrating radar. *Applied Engineering in Agriculture* 21(1): 71-87.

Allred, B.J., N.R. Fausey, J.J. Daniels, C-C. Chen, L. Peters., and H.S. Youn, 2004b. GPR detection of drainage pipes in farmlands. Proceedings of the Tenth International Conference Ground Penetrating Radar, GPR 2004, Delft, The Netherlands. Vol 1, Pp. 307-310.

Allred, B.J., N.R. Fausey, Jr., L. Peters, C. Chen, J.J. Daniels, and H. Youn, 2004. Detection of buried agricultural drainage pipes with geophysical methods. *Applied Engineering in Agriculture* 20(3): 307-318.

Allred, B.J., N.R. Fausey, J.J. Daniels, C-C. Chen, L. Peters., and H.S. Youn, 2003. Considerations for using ground penetrating radar to locate buried agricultural drainage pipe. Paper No. 032344. St Joseph, Michigan, American Society of Agricultural Engineers

Allred, B.J., and J.D. Redman, 2010. Location of agricultural drainage pipes and assessment of agricultural drainage pipe conditions using ground penetrating radar. *Journal of Environmental and Engineering Geophysics* 15(3): 119-134.

Cassidy, N.J., 2009. Electrical and magnetic properties of rocks, soils, and fluids. In *Ground Penetrating Radar: Theory and Applications*, ed. H. M. Jol, 41-72 pp. Elsevier Science, Amsterdam, The Netherlands.

Chow, T.L., and H.W. Rees, 1989. Identification of subsurface drain locations with ground-penetrating radar. *Canadian Journal of Soil Science* 69: 223-234.

Corwin, D.L., 2008. Past, present, and future trends in soil electrical conductivity measurements using geophysical methods. In *Handbook of Agricultural Geophysics*, ed. Allred, B. J., J .J. Daniels and M. R. Ehsani, 17-44 pp. CRC Press, Taylor and Francis Group, Boca Raton, Florida.

Daniels, D.J., 2004. *Ground Penetrating Radar; 2nd Edition*. The Institute of Electrical Engineers, London, United Kingdom.

Davis, J.L., and A.P. Annan, 1989. Ground-penetrating radar for high-resolution mapping of soil and rock stratigraphy. *Geophysical Prospecting* 37: 531-551.

Doolittle, J.A., R.D. Windhorn, D.L. Withers, S.E, Zwicker, F.E. Heisner and B.L. McLeese, 2008. Soil Scientists Revisit a High-Intensity Soil Survey in Northwest Illinois with Electromagnetic Induction and Tradition Methods. *Soil Survey Horizons* 49(4):102-108.

Grasmueck, M., and A.G. Green, 1996. 3-D georadar mapping: Looking into the subsurface. *Environmental and Engineering Geoscience*, Vol II (2): 195-220.

Geonics Limited, 2007. EM38-MK2 ground conductivity meter operating manual. Geonics Ltd., Mississauga, Ontario.

Greenhouse, J.P. and D.D. Slaine, 1983. The use of reconnaissance electromagnetic methods to map contaminant migration. *Ground Water Monitoring Review* 3(2): 47-59.

Jaynes, D.B., 1995. Electromagnetic induction as a mapping aid for precision farming. pp. 153-156. IN: Clean Water, Clean Environment, 21st Century: Team Agriculture. Working to Protect Water Resources. Kansas City, MO. 5 to 8 March 1995.

Jol, H., 2009. *Ground Penetrating Radar: Theory and Applications*. Elsevier Science, Amsterdam, The Netherlands.

Kachanoski, R.G., E.G. Gregorich and I.J. van Wesenbeeck, 1988. Estimating spatial variations of soil water content using noncontacting electromagnetic inductive methods. *Canadian Journal of Soil Science* 68:715-722.

Lehmann, F., and A.G. Green, 1999. Semiautomatic georadar data acquisition in three dimensions. *Geophysics*, 64(3): 719-731.

Lück, E., R. Gebbers, J. Ruehlmann and U. Sprangenberg, 2009. Electrical conductivity mapping for precision farming. *Near Surface Geophysics*. 7(1): 15-25.

McNeill, J.D. 1980. Electrical conductivity of soils and rock; Technical Note TN-5: Geonics Limited, Mississauga, Ontario, Canada.

Rhoades, J.D., P.A. Raats and R.J. Prather, 1976. Effects of liquid-phase electrical conductivity, water content, and surface conductivity on bulk soil electrical conductivity. *Soil Science Society of America Journal* 40:651-655.

Rogers, M.B., J.R. Cassidy, and M.I. Dragila, 2005. Ground-based magnetic surveys as a new technique to locate subsurface drainage pipes: A case study. *Applied Engineering in Agriculture* 21(3): 421-426.

Zeng X., and G.A. McMechan, 1997. GPR characterization of buried tanks and pipes. *Geophysics* 62: 797-806.